PHYSICAL REVIEW A VOLUME 22, NUMBER 5 NOVEMBER 1980

Time-of-flight study of H(2S) and D(2S) produced by electron impact on H_2 and D_2: Fast peaks

J. J. Spezeski, O. F. Kalman, and L. C. McIntyre, Jr.
Department of Physics, University of Arizona, Tucson, Arizona 85721
(Received 8 February 1980)

Time-of-flight spectra of H(2S) and D(2S) fragments from electron-bombardment dissociated H_2 and D_2 have been observed. Kinetic energy distributions of "fast" metastable fragments were obtained for electron-bombardment energies ranging from near the threshold for fast metastable production (less than 29 eV) to 100 eV. At low bombarding energies previously unreported structure is observed in the fast peaks for both isotopes. At high bombarding energies also there is evidence of unresolved structure in the fast peaks. The present data are compared with the results of earlier investigations. At low bombarding energies there are significant discrepancies between the present results and previous measurements. At high bombarding energies there is significant disagreement with a calculation that assumes a single dissociating state. The observed shift of the fast peak as a function of the bombarding electron energy is compared to predictions incorporating a form of the Wannier law. This comparison tends to confirm the presence of more than one dissociation channel yielding fast metastables. Several excited states of H_2 and H_2^+ are discussed as possible dissociation channels contributing to the observed kinetic energy distributions.

I. INTRODUCTION

Metastable H(2S) fragments resulting from electron-bombardment-induced dissociation of H_2 have been reported by several investigators.[1-7] Typically, two distinct energy groups of H(2S) atoms are observed: a "fast" group centered at about 5 eV, and a "slow" group with energies peaked at about 0.3 eV. In a previous paper[1] we presented a time-of-flight (TOF) study of the slow metastables from the molecular species H_2, D_2, and HD showing partially resolved structure caused by predissociation from bound vibrational levels of excited molecular states. In the present paper we report a TOF study that concentrates on the fast H(2S) and D(2S) fragments from the dissociation of H_2 and D_2.

Leventhal *et al.*[7] suggested that doubly excited molecular states were responsible for the fast metastables. Misakian and Zorn[4] concluded that the dominant state was a $Q_2\,^1\Pi_u$ doubly excited state that dissociates into H(2S)+H(2P). Their assignment was based on measurements of the angular distribution and excitation function of H(2S) metastables coming from dissociations of H_2, and they did not explicitly consider the possibility that more than one state was involved.

There have been some discrepancies among the several studies of the fast peak. Leventhal, Robiscoe, and Lea[7] reported a double fast peak appearing when fragments were observed at a 77° angle relative to the electron beam. Misakian and Zorn[4] reported no such double fast peak at any angle from 60–120°. In addition there has been disagreement concerning the shape and position of the kinetic energy distribution of the fast metastables. Hazi and Wiemers[8] compare their calculated fragment distributions, which assume only $Q_2\,^1\Pi_u$ participation, with three separate measurements[3,4,7] of the velocity distribution of fast hydrogen and deuterium metastables. They conclude that there are significant discrepancies between their calculations and existing measurements that are not simply explained as the effects of momentum transfer from the bombarding electron or the result of the thermal motion of the target molecules. The calculation of Hazi and Wiemers considered dissociations of only the $Q_2\,^1\Pi_u$ state and did not allow for dependence of the velocity distribution on electron bombarding energy (EBE). The present study shows that near threshold the fast peak shifts significantly with EBE. Moreover, we find several indications that there is more than a single dissociation channel contributing to the fast peak.

II. EXPERIMENTAL

To study the fast metastables a microwave quench cavity was added to the apparatus described in our previous study of slow metastables[1] and the solid angle of the Lyman-α detector was increased. A diagram of the present apparatus is shown in Fig. 1. A pulsed electron beam intersects a collimated beam of thermal H_2 or D_2 molecules. Metastable 2S fragments from resulting dissociations traverse a measured flight path and are quenched in a dc electric field present at the quench plates.[9] The resulting Lyman-α radiation is detected by two channel-electron multipliers (CEM's). A clock is started when the electron gun is pulsed and stopped when a CEM pulse is detected. The distribution of these flight times is then accumulated. A second CEM was added op-

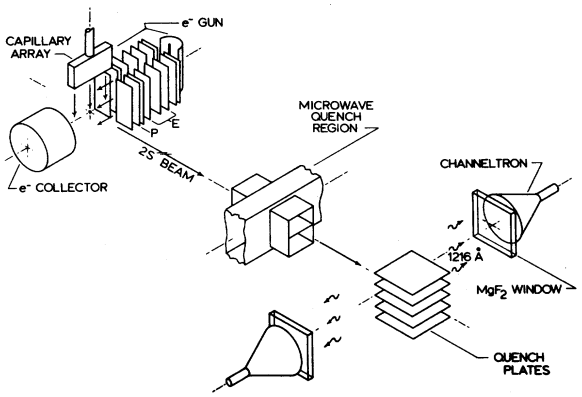

FIG. 1. Schematic apparatus diagram. The pulsed grid in the electron gun, consisting of a fine mesh covering a vertical slit, is labeled P; a three-element einzel lens is labeled E. The vertical molecular beam is shown intersecting the horizontal electron beam. The microwave quench region and the two CEM Lyman-α detectors are also shown.

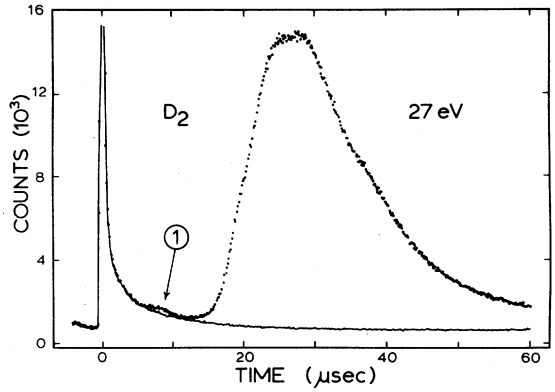

FIG. 2. TOF distribution of D(2S) fragments from D_2 showing the "slow peak" and the much smaller "fast peak" (near 8 μsec). The background distribution is shown as a solid line and the signal plus background data are shown as points. The nominal electron bombarding energy was 27 eV with ±2-eV energy spread. The numbered features are discussed in the text.

posite the one used previously and the size of the CEM input cones was increased from 1.0 to 2.5 cm. This resulted in a tenfold increase in signal strength over the previous arrangement. The microwave quench cavity, which is fully described in Ref. 10, consisted of a section of x-band waveguide located between the metastable source and Lyman-α detector with openings through which the metastable beam could pass. A standing microwave electric field at a frequency of 9.9 GHz (corresponding to the $2S_{1/2}$ to $2P_{3/2}$ transition in H or D) could be introduced into the waveguide by a logic signal from our data taking system. The microwaves effectively quench the metastable 2S fragments (and only the 2S fragments) well ahead of the Lyman-α detector allowing us to obtain a good measurement of the background. The background spectrum probably originates from photons from excited atomic and molecular states produced by the electron pulse. These photons have no direct path to the CEM because of shields between the CEM entrance cone and the source, however they could undergo one or more reflections and arrive at the CEM. During a typical measurement we alternated between microwave on and off data every 500 sec and accumulated background and signal plus background spectra in separate sections of our analyzer memory. Figure 2 illustrates the need for the background measurement for EBE near the threshold for formation of fast metastables. The fast D(2S) signal near 8 μsec in Fig. 2 is only a small fraction of the background signal for a 27-eV EBE. Other data features of Fig. 2 that should be noted are (i) the "prompt" peak corresponding to the electron pulse and defining the origin of the TOF axis, and (ii) the broad slow peak at 26 μsec arising from dissociations and predissociations of singly excited states (see Ref. 1).

Data for the present study, unless clearly stated otherwise, were taken with the electron beam at 90° to the flight path of the detected metastable fragments. The electron pulse width was 0.10 μsec and the time-bin width in our collected TOF spectra was 0.125 μsec/channel. The electron pulse rate was 5 kHz for H_2 and 3.4 kHz for D_2. The time-averaged electron current ranged from 0.05 to 0.3 μA depending on the bombarding voltage. Due to the voltage drop across the directly heated filament the energy spread of the electron beam was about ± 2 eV. The flight path measured from the center of the source to the leading edge of the detector plates was 18.3 ± 0.1 cm. The spatial extent of the source region was about 0.2 cm along the flight path. The extent of the quench region associated with the Lyman-α detector was about 0.05 cm along the flight path.[9] The background pressure in our vacuum chamber was about 1×10^{-5} Torr when the metastable source was operating.

III. RESULTS

The TOF spectra for fast 2S metastable fragments from H_2 and D_2 for various electron bombarding energies are shown in Figs. 3 and 4. The microwave-on background spectra have been subtracted to obtain the data in these figures. Typical run times ranged from 17 to 70 hours depending on the count rate, which, of course, depended on the

EBE. Typical combined count rates (from both the fast and slow peaks) ranged from about 30 to 200 counts/sec. The corresponding energy spectra, obtained by a straightforward numerical conversion, are shown in Figs. 5 and 6. Three features in the data that will be discussed below are identified in the figures by arbitrary numbers 1–3. These features and the processes leading to them will be referenced in the remainder of the text by these numbers.

The accuracy of our energy measurement is limited by the calibration accuracy of the TOF axis. Values for TOF for the present results are valid to ± 0.06 μsec, which is the estimated error in the determination of time-zero and corresponds to an uncertainty of half the time-bin width. The associated uncertainty in energy E is proportional to $E^{3/2}$ and has the value ± 0.14 eV at $E = 6$ eV. The uncertainty in energy due to uncertainty in the flight path is smaller than that due to the time-zero uncertainty. Some data were accumulated for HD but are not included in the present paper because the H(2S) and D(2S) features are not completely resolved by the present apparatus thereby complicating the task of determining peak positions and shapes. Also, in contrast with the results of our slow-peak study,[1] the fast-peak energy spectra for HD were not strikingly different from the H_2 and D_2 results. For HD we observed the ratio of fast H(2S) to fast D(2S) fragments to be 1.09 ± 0.05. This is in reasonable agreement with the 1.21 ± 0.12 ratio reported by Carnahan and Zipf.[2]

For H_2 and D_2, the low-energy side of the fast peak overlaps with the high-energy side of the slow peak. This overlap is noticeable for EBE below about 38 eV where the fast peak is small relative to the slow peak (see Fig. 2). The overlap is clearly seen in the low EBE data of Figs. 5 and 6. The following formula for converting time to energy (for a 18.3-cm flight path) is useful for examining corresponding features in the time and energy spectra:

$$E = 174.6\, M/T^2, \tag{1}$$

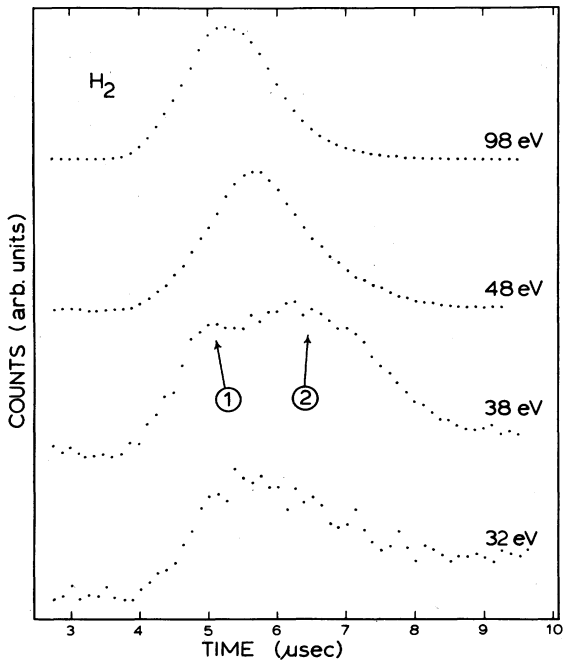

FIG. 3. TOF distributions of fast H(2S) metastables from H_2 for several electron bombarding energies. The numbered features are discussed in the text.

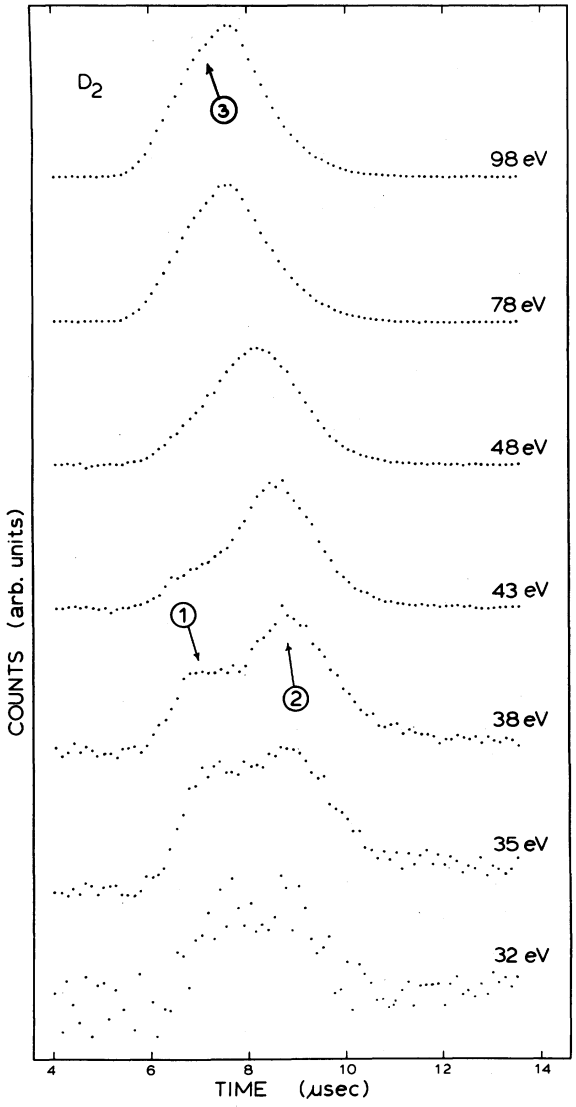

FIG. 4. TOF distributions of fast D(2S) metastables from D_2 for several electron bombarding energies. The numbered features are discussed in the text.

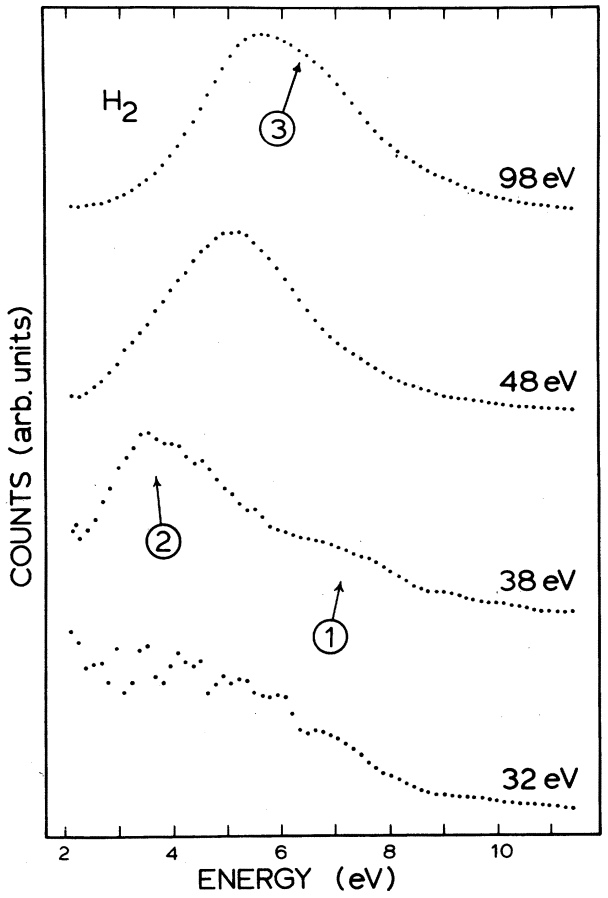

FIG. 5. Energy distributions of fast H(2S) metastables from H_2 for several electron bombarding energies. The numbered features are discussed in the text.

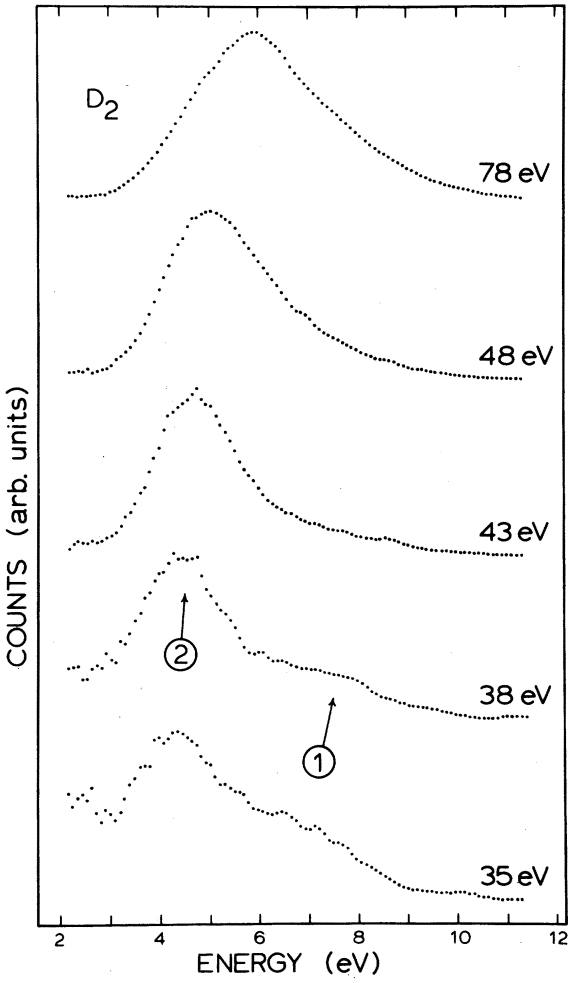

FIG. 6. Energy distributions of fast D(2S) metastables from D_2 for several electron bombarding energies. The numbered features are discussed in the text.

where E is the fragment energy in eV, M the fragment mass number, and T the time-of-flight in μsec.

Several aspects of the data warrant special note. One is the shift of the peak position to shorter times (higher energies) as the EBE is increased. For any single dissociation channel such a shift could be explained in part as an excess energy effect such as that described by the Wannier Law.[11] This explanation is pursued further in the next section. There is also the appearance of two partially resolved bumps (features 1 and 2) in the data below 40 eV. A third aspect is the bulge (feature 3) on the short-time (high-energy) side of the fast peaks for 98 eV. This structure in the fast peaks, which has not been reported previously, is also considered further in the Sec. IV. Finally, it can be seen in Fig. 2 that fast metastables (3–6 eV) are clearly present in our 27-eV data. This may be significant because Misakian and Zorn[4] reported a 29-eV threshold for 2-eV 2S fragments.

To confirm our results for D_2 we acquired a series of TOF spectra after making the following changes in our apparatus. The flight path was reduced to 11.8 cm and the electron pulse and TOF bin width were widened to 0.25 μsec. This reduced our resolution but gave us a much higher count rate. In addition we returned to using a single CEM to exclude any artifacts possibly coming from our former two-CEM operation. We acquired TOF data from 27.6 to 39.6-eV EBE in increments of roughly 2 eV and found that the fast-peak structure at these low EBE was reproducible.

In another auxiliary measurement we examined the distribution of H(2S) fragments from H_2 at an angle of 77° for 60-eV EBE. We found as did Misakian and Zorn[4] a single fast peak and not the double peak reported by Leventhal *et al.*[7]

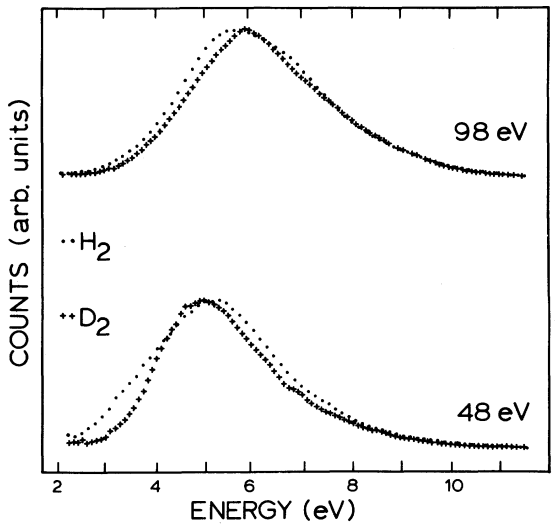

FIG. 7. Comparison of the metastable energy spectra for H_2 and D_2 for two electron bombarding energies. ••• H(2S) fragments from H_2; + + + D(2S) fragments from D_2.

IV. DISCUSSION

A. Comparisons

It is interesting to compare the H_2 and D_2 energy spectra. One expects similar results because the electronic structure is the same for the two molecules; however, there may be dissimilarities arising from the mass difference. Figure 7 compares the metastable energy spectra for H_2 and D_2 for two values of EBE. In both cases the D(2S) curve is slightly within the H(2S) curve which is probably a result of the narrower Franck-Condon region for D_2 than for H_2. The D(2S) peaks in Fig. 7, however, are less than 16% narrower than the H(2S) peaks as one would expect from a simple comparison of the widths of the Franck-Condon regions for the ground states of D_2 and H_2.

Figures 8–10 compare the present results with some earlier measurements and a calculation.[12] For such comparisons, of course, it is important that certain parameters of the experiment or model be similar. Most important is the EBE, especially at values near the threshold for metastable production. This is a consequence of the excess energy effect for any given dissociation channel and the opening of new channels as the EBE is increased. The angle of detection affects the fast-peak position significantly as has been shown for H^+ fragments by Van Brunt.[13] The effect of momentum transfer from the bombarding electron to the target molecule, which depends on both the EBE and detection angle, is relatively minor for the fast peak. The effective temperature or, equivalently, the initial velocity distribution of the target molecules also has only minor consequences for fast metastable spectra, although for slow metastables the reverse is true.[1] The data compared below were obtained for similar EBE and for a detection angle of 90° except for the data of Misakian and Zorn, which was obtained at 80°. Sharp features in the derived spectra are artifacts of our energy conversion arising from noise in the original data. The spectra are normalized to the same peak height. The error bars for the ex-

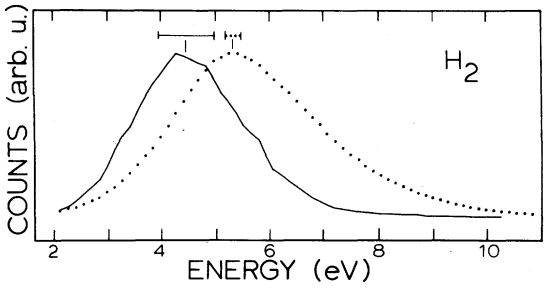

FIG. 9. Comparison of two experimental energy distributions of H (2S) from H_2. ••• Present results for 70-eV EBE; — results of Misakian and Zorn (Ref. 4) for 70-eV EBE.

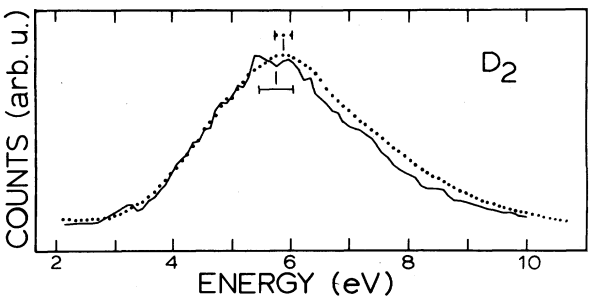

FIG. 8. Comparison of two experimental energy distributions of D(2S) from D_2. ••• Present results for 78-eV EBE; — results of Czuchlewski and Ryan (Ref. 3) for 80-eV EBE.

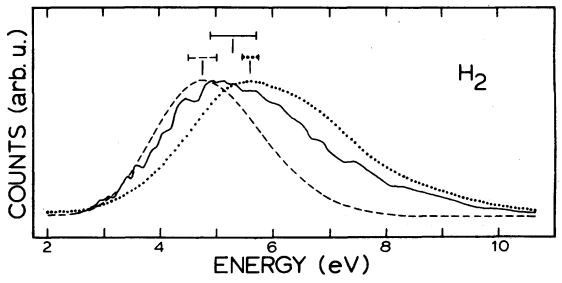

FIG. 10. Comparison of experimental and theoretical energy distributions of H(2S) from H_2. ••• Present measurements at 98-eV EBE; --- calculation of Hazi (Ref. 14) for 100-eV EBE; — results of Carnahan and Zipf (Ref. 2) for 100-eV EBE.

perimental results show the estimated error in the peak position due to uncertainties in time and length measurements. The uncertainty for the calculation was taken directly from Ref. 8.

Figure 8 compares the present D(2S) results with those of Czuchlewski and Ryan[3] for similar conditions. The two energy spectra shown are in substantial agreement as are also the H(2S) spectra of both investigations, which are not shown. Figure 9 compares present H(2S) results at 90° with those of Misakian and Zorn at 80° (Ref. 4). The difference in angle is too small to have a significant effect on the energy distributions. There appears to be some disagreement in these two measurements in that the positions of the maxima differ by about 1 eV, which is slightly larger than the combined uncertainty estimates. There can be no comparison of D(2S) results as Misakian and Zorn did not report any D(2S) measurements.

Figure 10 compares present results for 98-eV EBE with the 100-eV data of Carnahan and Zipf[2] and with a calculated H(2S) spectrum due to Hazi.[14] The measured spectra differ slightly in peak position but have similar shape. The calculated distribution, however, is significantly different in shape from the measured distributions. A comparison of our D(2S) results with Hazi's shows a similar discrepancy in the shape of the fast peak. Because of the basic agreement of present and previous measurements concerning peak shape, and because of our lack of any reason to suspect a serious error in the calculation, we conclude that the discrepancy indicates that states other than the $Q_2\,^1\Pi_u$ contribute to the fast metastable spectrum. Several possible states are discussed in Sec. IV B.

We consider next the observed shift in the fast-peak position as the EBE is increased from a value near threshold. It is easy to see that at EBE's very near threshold it is energetically impossible to produce the highest energy fragments observed at EBE's far above threshold. Specifically, the kinetic energy released in the molecular dissociation plus the separated atom energy (above the ground state) cannot exceed the electron bombarding energy. This can be pursued further by applying the excess energy relationship of Wannier.[11] For electron bombardment of H_2 leading to dissociative excited states of H_2 or H_2^+ that can yield 2S fragments this relationship would state that within several eV of the threshold for producing a 2S fragment with energy E (total released energy is $2E$) the cross section for production is proportional to a power (near 1) of the excess EBE above threshold. The threshold electron energy E_t depends on E and is given by

$$E_t = E_d + 2E\,, \tag{2}$$

where E_d is the internuclear potential at the separated-atom limit, i.e., the dissociation energy for the molecular state in question. It is instructive to include the excess energy effect in a calculation of the metastable energy distributions as a function of EBE even though such a calculation stretches the limit of validity of the Wannier law. Dunn and Kieffer[15] used a linear excess energy law to model the energy distribution of fast proton fragments produced by electron bombardment of H_2 and they found it to be a reasonable approximation up to EBE on the order of 70 eV, i.e., up to about 50 eV in excess of the dissociation threshold. We have performed a calculation of the distribution of H(2S) fragments from electron-bombardment-induced dissociation of H_2 incorporating the excess energy effect mentioned above and the following additional simplifying approximations: (i) Only the $Q_2\,^1\Pi_u$ excited state yields fast metastables; (ii) a Morse function approximates the ground state wave function; (iii) the excited state wave function is an appropriately normalized and positioned delta function, i.e., the Winans-Stueckelberg approximation[16]; and (iv) the probability for producing a metastable fragment with a given energy is proportional to a Franck-Condon factor times an excess energy factor. The internuclear potential for the $Q_2\,^1\Pi_u$ state was taken from Ref. 8. We did not include any averaging over the thermal velocities of the target molecules, nor any momentum transfer effects. Also omitted was the effect of autoionization. For simplicity we assumed an electron energy distribution that was square (instead of, for example, Gaussian) with a width of 4 eV and centered at the nominal value of EBE. The spectra thus calculated are shown in Fig. 11.

One conclusion we draw is that the observed shift in the location of the fast peak as a function of EBE is largely due to an excess energy effect.

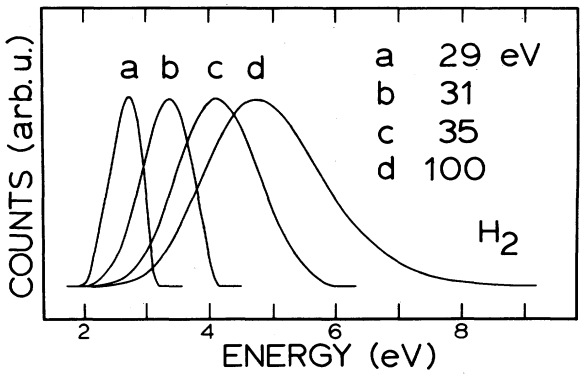

FIG. 11. Calculated approximate H(2S) energy distributions for various electron bombarding energies for the $Q_2\,^1\Pi_u$ excited state.

This has also been suggested by Hazi and Wiemers.[8] Calculations of the fast-peak energy distribution, therefore, should include the dependence of the production cross section via a specific channel upon the electron impact energy, at least for EBE within about 30 eV of the production threshold for that channel. For EBE of roughly 70 eV above threshold and higher, the excess energy effect can safely be ignored. It should be noted that for Fig. 10 we compared Hazi's calculation, which omits any dependence on excess energy, with our data for EBE = 98 eV, which is in the region where the dependence would have been minor. Another important thing to note is that in Fig. 11 the distributions are much narrower for low EBE than for high. This is contrary to our observations for the fast metastable peaks from H_2 and D_2. We interpret this discrepancy as another indication that there are several dissociation channels yielding fast 2*S* fragments.

We discuss next the discrepancy between the present observation of 3–6 eV metastables at an EBE of 27 eV (see Fig. 2) and the previous report by Misakian and Zorn[4] of a 29-eV EBE threshold for 2-eV fragments. The present electron gun and data do not allow a good determination of the threshold EBE, but they do allow us to make a reasonable choice between two general explanations for the fast metastables shown in Fig. 2. The first explanation, which we reject, is that there was a significant current of electrons in the energy range 31–37 eV or higher that excited some molecular state or states that then dissociated to the $2S+2l$ limit of 24.9 eV. The possibility of many 31–37 eV electrons from our gun, which had a nominal EBE of 27 eV and an energy spread of ±2 eV, is remote. The second explanation, which we prefer, is that the nominal EBE is correct and that the 3–6 eV fragments came from excited molecules dissociating to the $1S+2S$ limit at 14.8 eV. This explanation leads to a more plausible interpretation of the data for all EBE and is pursued in Sec. IV B.

There is another discrepancy between the present results and those of Misakian and Zorn that may be related to the discrepancy in apparent threshold for the fast metastables. Misakian and Zorn[4] reported that the least energetic of the fast H(2*S*) atoms have a kinetic energy of slightly in excess of 2 eV, and their Fig. 14 shows no H(2*S*) fragments with energies between 1–2 eV for an EBE of 40 eV. In contrast, we observe relatively large numbers of 1–2 eV metastables for 38 eV electrons. Our data at and below 38 eV, as mentioned previously, show a clear overlap of the fast and slow peaks and not the separation of these peaks that Fig. 14 of Ref. 4 indicates. The detector used by Misakian and Zorn was sensitive to more kinds of background than the present off-axis Lyman-α detector. They also used a 0.5-μsec electron pulse whereas we used a 0.1-μsec pulse. These differences in apparatus may partially explain the discrepancies mentioned above and may also have made it more difficult for Misakian and Zorn to resolve the fast-peak structure we observe.

B. Metastable production channels

Previously only the $Q_2\,{}^1\Pi_u(1\pi_u 2\sigma_g)$ doubly excited state of H_2 has been strongly proposed as a channel

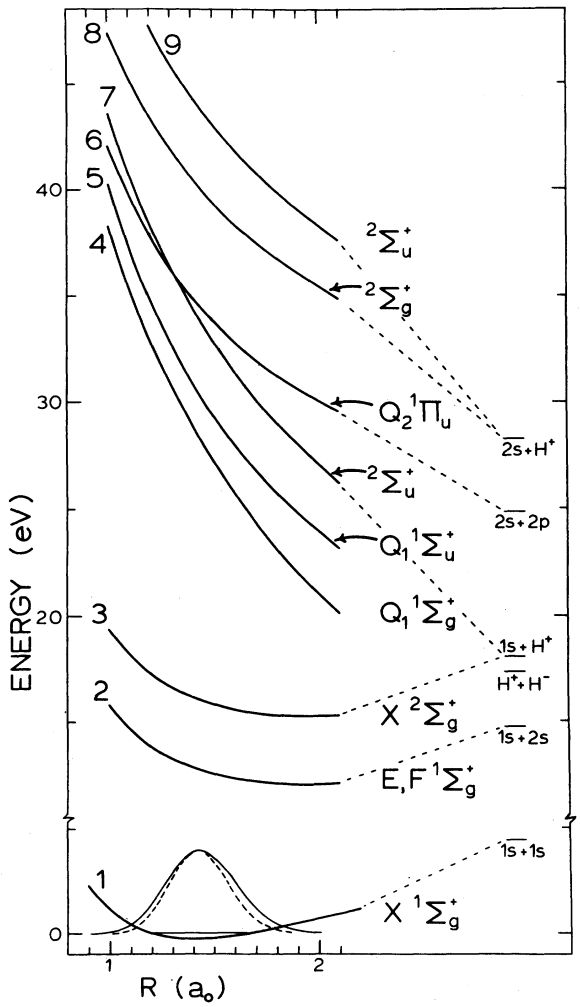

FIG. 12. Potential energy curves for selected states of H_2 and H_2^+. 1: $H_2 X\,{}^1\Sigma_g^+(1\sigma_g^2)$ from Ref. 17; 2: H_2^* E, $F\,{}^1\Sigma_g^+(1\sigma_g 2\sigma_g)+(1\sigma_u^2)$ from Ref. 17; 3: $H_2^*\,{}^2\Sigma_g^+(1\sigma_g)$ from Ref. 17; 4: H_2^{**} $Q_1\,{}^1\Sigma_g^+(1\sigma_u^2)$ from Ref. 18; 5: $H_2^{**}\,Q_1\,{}^1\Sigma_u^+$ $(1\sigma_u 2\sigma_g)$ from Ref. 19; 6: $H_2^{**}\,Q_2\,{}^1\Pi_u(1\pi_u 2\sigma_g)$ from Ref. 8; 7: $H_2^+\,{}^2\Sigma_u^+(2\sigma_u)$ from Ref. 17; 8: $H_2^+\,{}^2\Sigma_g^+(2\sigma_g)$ from Ref. 17; 9: $H_2^+\,{}^2\Sigma_u^+(2\sigma_u)$ from Ref. 17. The vibrational probability distribution is shown for the ground state of H_2 (solid curve) and D_2 (dashed curve).

for the production of fast 2S fragments at an angle of 90° (Ref. 4). Leventhal *et al.*[7] considered the $^{1,3}\Sigma_u^+(1\sigma_u 2\sigma_g)$ states, but these were later ruled out by Misakian and Zorn[4] because of symmetry arguments. Hazi and Wiemers,[8] who first calculated 2S energy distributions from the $Q_2\,^1\Pi_u$ state, do not mention some important implications of their calculated $Q_2\,^1\Pi_u$ potential curve concerning the production threshold for fast metastables. Based on their potential curve and on the ground-state wave function for H_2, one would expect the lowest 2S fragment energy to be about 3.1 eV and the threshold for these fragments to be 31 eV. Yet Misakian and Zorn[4] previously reported a 29 eV threshold for 2-eV fragments and attributed these fragments to the $Q_2\,^1\Pi_u$ state. Thus even before the present observations of structure in the fast peak, there was good reason to consider channels other than the $Q_2\,^1\Pi_u$ state. The discussion below considers several excited states of H_2 and H_2^+ in the order of their approximate expected threshold energy. Potential energy curves for states relevant to the discussion are shown in Fig. 12. Triplet states are not considered because, in general, a particular triplet will be important for 2S production only if the corresponding singlet is important. Calculations by Khare[20] for excitation of H_2 by electron impact support the general conclusions that cross sections for excitation to triplets tend to rise more sharply at threshold, peak at lower EBE, and fall off more rapidly than cross sections for excitation to singlets. Thus one might expect 2S production via an excited state of a particular symmetry to proceed primarily through the triplet state of that symmetry only near threshold. For EBE more than about 10 eV above threshold, the singlet state should be dominant in producing metastable fragments.

1. Symmetry considerations. Excitation cross sections are not currently available for the doubly excited states possibly involved in 2S production, and calculating such cross sections is a difficult task. Therefore symmetry arguments and selection rules can be useful for assessing whether production channels with particular symmetries and quantum numbers are likely or unlikely. For electron bombardment these kind of arguments are typically only approximately valid and care should be taken not to abuse them. Dunn[21] pointed out the presence and significance of anisotropies in the angular distributions of molecular dissociation products. Under certain conditions the direction of the incident electron $\vec{k}$ is a symmetry axis of the electron-molecule system. The excitation probability then depends, in general, on the relative orientation of $\vec{k}$ and the instantaneous direction of the internuclear axis $\vec{R}$. If the dissociation is rapid relative to a rotational period the dissociation fragments travel along the same instantaneous direction of $\vec{R}$. Dunn applied symmetry arguments to many possible transitions for perpendicular and parallel molecular orientations and deduced that certain transitions were forbidden for one or both of these orientations. For the present problem in which the initial state has Σ_g^+ symmetry and the observation angle is perpendicular to the incident electrons, the final-state symmetries for which the transition probability is not forbidden are Σ_g^+, Π_u, and Δ_g. The foregoing conclusion is exact at the threshold EBE but, as Dunn and Kieffer have noted,[15] it rapidly breaks down as the EBE increases above threshold. Above threshold the momentum change vector $\vec{K}$ of the scattered electron is the symmetry axis and many orientations of $\vec{K}$ are possible. At threshold $\vec{K}$ is aligned with $\vec{k}$. However, at only 17 eV above threshold the most probable direction for $\vec{K}$ is shifted about 40° away from $\vec{k}$ (Ref. 15).

The validity of simple symmetry arguments and the dipole-Born approximation for predicting angular distributions has been discussed by Van Brunt.[22] He states that generally there may be no laboratory angle at which the fragment intensity vanishes for EBE above threshold. Van Brunt also points out the importance of multipole terms other than the dipole term near threshold. Thus, for example, the dipole selection rules, $g \not\to g$ $\Delta\Lambda = 0, \pm 1$, cannot be applied at the threshold for electron-bombardment excitation. Because of the limitations to symmetry arguments and selection rules for the present problem, we will not be overly concerned with them in the following discussion. We will be more concerned with whether the expected threshold and calculated energy distribution for a specific channel are consistent with our measurements. For excited neutral molecules we will also be concerned with autoionization probabilities.

2. Data for 27 eV. First we consider the source of the fast 2S fragments observed at 27-eV EBE (see process 1 in Fig. 2). There are two known doubly excited states that might yield fast metastables at this EBE: The $Q_1\,^1\Sigma_g^+(1\sigma_u^2)$ and the $Q_1\,^1\Sigma_u^+(1\sigma_u 2\sigma_g)$. The $Q_1\,^1\Sigma_g^+$ state is symmetry-allowed (at 90° at threshold) and has been cited as a prominant channel in the dissociative excitation of H_2 leading to fast ion[23,24] and fast high-Rydberg fragments.[25,26] About 11–14% of excited $Q_1\,^1\Sigma_g^+$ molecules fail to autoionize and separate into two neutral fragments or H^+ and H^- (Ref. 8). A possible mechanism proposed by Schiavone *et al.*[26] for $H(nl, n>15)$ production via this state is the following. The excited $Q_1\,^1\Sigma_g^+$ molecule dissociates along the repulsive potential curve and fails to autoionize before reaching the stabilization dis-

tance (the distance at which the potential curve for the doubly excited state crosses the curve for the ground state of the ion). It continues to dissociate reaching the $(1\sigma_g n l\lambda)$ series of Rydberg states converging to the H_2^+ ground state. The molecule jumps to a Rydberg curve and completes the dissociation along this curve yielding a Rydberg fragment. There are difficulties extending this mechanism to $n=2$ to account for 2S production. The $Q_1\,^1\Sigma_g^+$ internuclear potential calculation by Bottcher and Docken[18] excludes the ground-state configuration $(1\sigma_g^2)$ and is not reliable at large internuclear distances R. The projected atomic orbitals (PAO) curve of O'Malley[19] is more accurate at large R and has an avoided crossing with the $E,F(1\sigma_g 2\sigma_g)+(1\sigma_u^2)$ curve in the neighborhood of 8 bohr. If a jump to the E,F curve occurs then a 2S fragment will be produced as the dissociation is completed along the E,F curve, which has a separated atom limit of $1S+2S$. It is not clear whether such a curve jump is likely. However, the expected energy distribution (calculated in a way similar to the distributions in Fig. 11) and threshold (about 23 eV) are consistent with our data and thus make the $Q_1\,^1\Sigma_g^+$ state a good possibility for process 1.

The $Q_1\,^1\Sigma_u^+(1\sigma_u 2\sigma_g)$ channel is symmetry-forbidden. This state dissociates into a combination of H(1S)+H(2S) and $H^+ + H^-$ (Ref. 27). However, according to a recent calculation by Kirby *et al.*[27] only about 3% of excited $Q_1\,^1\Sigma_u^+$ molecules dissociate. The other 97% of the molecules autoionize. Thus it appears unlikely that this state is an important production channel for fast metastables although it probably is a likely channel for proton production.[27-29] The expected energy distribution and threshold (about 25 eV) are consistent with our data. If $Q_1\,^1\Sigma_u^+$ and $Q_1\,^1\Sigma_g^+$ channels both exist and are active at 27 eV and higher EBE, it would be doubtful that their contributions are resolved.

3. Data near 38 eV. We next consider the double peak in the data near 38 eV. It seems reasonable that the peak discussed above (process 1) as possibly due to the $Q_1\,^1\Sigma_g^+$ state is still present although shifted to higher energy as a result of the excess energy effect. A second peak (process 2), which appears at a lower fragment energy than the first can arise from the doubly excited $Q_2\,^1\Pi_u$ $(1\pi_u 2\sigma_g)$ state. A calculation by Hazi and Wiemers[8] predicts that 86–90% of excited $Q_2\,^1\Pi_u$ molecules dissociate to H(2S)+H(2P). The expected threshold (about 31 eV) and energy distribution are consistent with our observations and excitation to this state is symmetry-allowed. Thus it seems likely that the second feature does come from the $Q_2\,^1\Pi_u$ state as previously suggested by Misakian and Zorn.[4] It should be pointed out that, although we agree with Misakian and Zorn that this is an important 2S production channel, we disagree with their experimental results for fast 2S atoms in several significant areas. Their reasoning concerning the $Q_2\,^1\Pi_u$ state hinged strongly on their measurements of the excitation function for 3.8-eV metastable fragments and on the angular distribution of 2S fragments at 41.5-eV EBE. Our observations of a possible threshold below 29 eV and structure in the fast peak for EBE in the neighborhood of 40 eV both cast doubt on the validity of their reasoning. Their conclusion that triplets are not important, which was also based on their measured excitation function, is likewise questionable if our 27-eV data are valid. In addition we note two discrepancies with their reported 29-eV threshold for 2-eV fragments. First, as stated above, 2-eV fragments are not expected in significant amounts from $Q_2\,^1\Pi_u$ molecules if the calculated potential curve of Hazi and Wiemers[8] is valid. Second, 1–2 eV fragments are observed in the present work in the high-energy tail of the slow peak (see, for example, the 13.2–18.7-μsec data in Fig. 2). In contrast, Misakian and Zorn[4] report no 1–2-eV metastable fragment.

4. Data for 98 eV. For our data at 98 eV there is a clear bulge (process 3) on the high-energy side of the fast peak. The location of this bulge is consistent with the energy distribution expected for 2S fragments formed by the dissociation of the $^2\Sigma_g^+(2\sigma_g)$ excited state of H_2^+. Excitation of this state is symmetry-allowed and the threshold for this channel would be about 37 eV. This bulge is not clearly evident in the data at 78 and 48 eV; however, fast 2S from the $^2\Sigma_g^+$ state probably are produced at these EBE but not yet produced in large quantities because of relatively small excess energy factors. The $^2\Sigma_u^+(2\sigma_u)$ state of H_2^+ also dissociates yielding a 2S fragment. This channel has a threshold of about 40 eV; however, it is symmetry-forbidden. Fragments from this channel would have a peak energy of about 7.5 eV for a 100-eV EBE, whereas fragments from the $^2\Sigma_g^+$ state would peak at about 5.7 eV at the same EBE. Our 98-eV data indicates that the $^2\Sigma_u^+$ channel is not very important at that EBE.

It is clear that, as one considers higher and higher EBE, more and more channels are open for fast metastable production. It is also clear that many doubly excited states that might be important to fast metastable production have not been treated theoretically; for instance, the potential energy curves may not be known. The L, M, and T doubly excited states of H_2 are good examples. Sharp[17] correlates each of these states with a separated atom limit involving H(2S), and Huber and Herzberg[30] list some experimental data for

each of them, but their internuclear potentials are unknown. It is also conceivable that there are H_2^- resonance states contributing to 2S production, but little is known about this possibility. The above discussion, which considered only states for which the potential curve was known, is readily acknowledged to be incomplete. Further theoretical work could be helpful. It seems especially important that calculations of energy distributions properly include an excess energy effect. Experiments in which both dissociation fragments are detected also show promise for being useful. Measurements of angular distributions beyond those already in existence may not be helpful because of the large number of channels yielding fast 2S fragments. Careful measurements of excitation functions, on the other hand, could be very useful.

V. SUMMARY

The problem of fast metastable production appears to be more complex than has been generally realized. Present measurements demonstrate the existence of at least three production channels and the possibility of several more cannot be eliminated. Identification of these channels is complicated by limitations in the available measurements and calculations. The energy distribution of metastable fragments from a specific channel and the relative importance of the channel depend significantly on the EBE. Two proposed channels involve the $Q_2\ ^1\Pi_u(1\pi_u 2\sigma_g)$ state of H_2 and the $^2\Sigma_g^+(2\sigma_g)$ state of H_2^+. A third channel with a threshold below 29 eV may involve the $Q_1\ ^1\Sigma_g^+(1\sigma_u^2)$ autoionizing state of H_2.

ACKNOWLEDGMENTS

The authors want to thank A. Hazi for sending us calculated energy distributions for our specific experimental conditions. We also thank A. Hazi and R. S. Freund for fruitful discussions. This research was sponsored by the Air Force Office of Scientific Research, Air Force Systems Command, USAF, under Grant No. 75-2864.

[1]S. R. Ryan, J. J. Spezeski, O. F. Kalman, W. E. Lamb, Jr., L. C. McIntyre, Jr., and W. H. Wing, Phys. Rev. A 19, 2192 (1979).
[2]B. L. Carnahan and E. C. Zipf, Phys. Rev. A 16, 991 (1977).
[3]S. J. Czuchlewski and S. R. Ryan, Bull. Am. Phys. Soc. 18, 688 (1973).
[4]M. Misakian and J. C. Zorn, Phys. Rev. A 6, 2180 (1972).
[5]J. W. Czarnik and C. E. Fairchild, Phys. Rev. Lett. 26, 807 (1971).
[6]R. Clampitt and A. S. Newton, J. Chem. Phys. 50, 1997 (1969).
[7]M. Leventhal, R. T. Robiscoe, and K. R. Lea, Phys. Rev. 158, 49 (1967).
[8]A. U. Hazi and K. Wiemers, J. Chem. Phys. 66, 5296 (1977).
[9]S. Czuchlewski, S. R. Ryan, and W. H. Wing, Rev. Sci. Instrum. 47, 1026 (1976).
[10]S. R. Ryan, S. J. Czuchlewski, and M. V. McCusker, Phys. Rev. A 16, 1892 (1977).
[11]G. H. Wannier, Phys. Rev. 90, 817 (1953).
[12]Spectra for Figs. 8–10, other than the present results, were derived from tables and enlarged figures provided by A. Hazi and E. Zipf.
[13]R. J. Van Brunt, Phys. Rev. A 16, 1309 (1977).
[14]A. Hazi, private communication. Hazi extended the results of Ref. 8 to cover the specific conditions of the present work.
[15]G. H. Dunn and L. J. Kieffer, Phys. Rev. 132, 2109 (1963).
[16]See, for example, G. Herzberg, *Spectra of Diatomic Molecules*, 2nd ed. (Van Nostrand, Princeton, N. J., 1950), p. 393. Footnote 13 of Ref. 8 shows the normalization explicitly.
[17]T. E. Sharp, At. Data 2, 119 (1971).
[18]C. Bottcher and K. Docken, J. Phys. B 7, L5 (1974).
[19]T. F. O'Malley, J. Chem. Phys. 51, 322 (1969).
[20]S. P. Khare, Phys. Rev. 149, 33 (1966); 152, 74 (1966); 157, 107 (1967).
[21]G. H. Dunn, Phys. Rev. Lett. 8, 62 (1962).
[22]R. J. Van Brunt, J. Chem. Phys. 60, 3064 (1974).
[23]A. Hazi, J. Chem. Phys. 60, 4358 (1974).
[24]K. Köllmann, J. Phys. B 11, 339 (1978).
[25]G. A. Khayrallah, Phys. Rev. A 13, 1989 (1976).
[26]J. A. Schiavone, K. C. Smyth, and R. S. Freund, J. Chem. Phys. 63, 1043 (1975).
[27]K. Kirby, S. Guberman, and A. Dalgarno, J. Chem. Phys. 70, 4635 (1979).
[28]S. Strathdee and R. Browning, J. Phys. B 9, L505 (1976).
[29]S. Strathdee and R. Browning, J. Phys. B 12, 1789 (1979).
[30]K. P. Huber and G. Herzberg, *Constants of Diatomic Molecules* (Van Nostrand, New York, 1978), pp. 244–246.